

Positron Radioactivities of O^{14} , Ne^{18} , Si^{26} , and S^{30}

G. FRICK, A. GALLMANN, D. E. ALBURGER,* D. H. WILKINSON,† AND J. P. COFFIN

Institut de Recherches Nucléaires, Strasbourg, France

(Received 22 July 1963)

A Siegbahn-Slätis intermediate-image spectrometer has been used to measure the positron spectra of the isotopes O^{14} , Ne^{18} , Si^{26} , and S^{30} produced by a He^3 beam from a 5.5-MeV Van de Graaff accelerator. O^{14} was formed in the $C^{12}(He^3, n)O^{14}$ reaction and it emits a positron group of $E_{max} = (4.085 \pm 0.030)$ MeV to the ground state of N^{14} and another group having $E_{max} = (1.821 \pm 0.007)$ MeV to the 2.3-MeV level. The branching ratios are $(0.65 \pm 0.05)\%$ ($\log ft = 7.23 \pm 0.04$) and $(99.35 \pm 0.05)\%$ ($\log ft = 3.49 \pm 0.01$), respectively. The measured half-life of O^{14} is 71.3 ± 0.1 sec. Ne^{18} was formed in the $O^{16}(He^3, n)Ne^{18}$ reaction and we find $E_{max} = (3.416 \pm 0.009)$ MeV to the ground state of F^{18} , and $T_{1/2} = 1.47 \pm 0.10$ sec. From a study of the beta and gamma rays of Ne^{18} by means of scintillation detectors we find a second positron branch feeding the 1.04-MeV level of F^{18} . The branching ratios obtained from these measurements are $(91 \pm 3)\%$ ($\log ft = 3.02 \pm 0.02$) to the ground state and $(9 \pm 3)\%$ ($\log ft = 3.47 \pm 0.13$) to the 1.04-MeV level. The isotope Si^{26} , produced by the $Mg^{24}(He^3, n)Si^{26}$ reaction, decays with two branches to Al^{26} . The more energetic branch feeds the 0.229-MeV isomeric state of Al^{26} and has $E_{max} = 3.828 \pm 0.013$ MeV from a magnetic spectrometer measurement, while the second branch is masked by other positron activities. We find $T_{1/2} = 2.1 \pm 0.1$ sec for Si^{26} . The second position branch of Si^{26} has been confirmed by observation of (0.820 ± 0.010) MeV gamma rays in coincidence with positrons. Branching ratios of Si^{26} , measured with scintillation detectors, are $(66.4^{+1})\%$ ($\log ft = 3.52_{-0.02}^{+0.04}$) for the branch to the 0.229 MeV level of Al^{26} and $(34.1^{+1})\%$ ($\log ft = 3.36_{-0.05}^{+0.02}$) for the branch to the 1.059-MeV level. S^{30} was produced by the $Si^{28}(He^3, n)S^{30}$ reaction and it decays with a half-life of 1.4 ± 0.1 sec and with positron branches of $E_{max} = (5.085 \pm 0.026)$ MeV to the ground state of P^{30} and $E_{max} = (4.422 \pm 0.022)$ MeV to the 0.684-MeV level. The branching ratios, obtained by analyzing the positron spectrum, are $(20 \pm 1)\%$ ($\log ft = 4.39 \pm 0.03$) and $(80.15^{+1})\%$ ($\log ft = 3.49_{-0.05}^{+0.09}$) respectively. Positron-gamma coincidence measurements have confirmed the decay scheme. Some comments are made on the abnormal value of the matrix element in the decay of O^{14} to the ground state of N^{14} and the results on the pure Fermi transitions observed in each of the isotopes are discussed.

INTRODUCTION

THE present work consists of studies of the positron radioactivities of the isotopes O^{14} , Ne^{18} , Si^{26} , and S^{30} , all having mean-lives of the order of seconds, with the help of a Siegbahn-Slätis intermediate-image focusing spectrometer. These isotopes were produced in the spectrometer by reactions induced by the He^3 beam from a 5.5-MeV Van de Graaff accelerator. A beam chopper and timing system allowed the measurements to be made only during the beam-off time.

 O^{14}

The nucleus O^{14} which has a ground state of $J^\pi = 0^+$ $T = 1$ (even-even nucleus) decays by positron emission to N^{14} . From the point of view of energetics, this decay can take place both to the ground state N^{14} and to the first excited state at 2.3 MeV. Since these two levels have spins and parities equal to $J^\pi = 1^+$ and 0^+ , respectively,¹ both transitions ought to be allowed by the selection rules.

The isotope O^{14} was first observed by Sherr, Muether, and White.² They measured the half-life as (76.5 ± 2) sec and by means of absorption techniques using Geiger-Müller counters they determined the maximum

energy of β_2^+ as (1.8 ± 0.1) MeV.³ They were also able to show that the β_2^+ of the O^{14} radioactivity is in coincidence with a gamma ray of 2.3 MeV which leads to the conclusion that this intense branch of positrons feeds the first excited state of N^{14} . The same authors also tried to obtain evidence for the transition β_1^+ to the ground state of N^{14} and they found for the intensity of this transition an upper limit of 5% relative to the transition to the first excited state of N^{14} . Subsequently J. B. Gerhart⁴ measured the spectrum of positrons from O^{14} by means of a magnetic spectrometer and obtained as the maximum energy an end-point of (1.835 ± 0.008) MeV. He measured the half-life of O^{14} with greater precision and found $T_{1/2} = (72.1 \pm 0.4)$ sec. Gerhart was not able to observe the positron transition to the ground state of N^{14} but pushed the limit of the relative branching to that state to a maximum value of 0.3%. Later, Sherr *et al.*⁵ repeated this same experiment but reported an actual value for this relative branch which they found to be equal to $(0.6 \pm 0.1)\%$. For such a value the $\log ft$ of the β^+ transition is 7.30 ± 0.07 . In all of these measurements the isotope O^{14} was produced inside a cyclotron by the reaction $N^{14}(p, n)O^{14}$. In order to study the properties of O^{14} the samples were transported by means of a special pneumatic system to the

* Permanent address: Brookhaven National Laboratory, Upton, New York.

† Permanent address: Nuclear Physics Laboratory, Oxford, England.

¹ F. Aijzenberg-Selove and T. Lauritsen, Nucl. Phys. **11**, 1 (1959).

² R. Sherr, H. R. Muether, and M. G. White, Phys. Rev. **75**, 282 (1949).

³ Throughout this paper β_1^+ is the highest energy positron branch, β_2^+ the first inner branch, etc. Except in the case of Si^{26} decay β_1^+ is the branch to the ground state.

⁴ J. B. Gerhart, Phys. Rev. **95**, 288 (1954).

⁵ R. Sherr, J. B. Gerhart, H. Horie, and W. F. Hornyak, Phys. Rev. **100**, 945 (1955).

detector which was in a location remote from the cyclotron.

R. Sherr *et al.*⁵ and recently K. Ott⁶ have made theoretical studies of the nuclei C^{14} , N^{14} , and O^{14} in order to interpret the small value of the O^{14} branching to the ground state of N^{14} . On the other hand various papers⁷⁻⁹ have appeared on the nucleus O^{14} from the point of view of the conserved-vector-current (CVC) theory. Thus, Bardin *et al.*⁷ made precision determinations of the Q values for the reactions $C^{12}(He^3, n)O^{14}$ and $C^{12}(He^3, p)N^{14}$ and they deduced from these measurements the maximum energy of the β^+ branch to the excited state of N^{14} as $E_2 = (1.8120 \pm 0.0014)$ MeV. The energy of the transition to the ground state of N^{14} therefore becomes $E_1 = 1.812 + 2.312 = (4.124 \pm 0.002)$ MeV. The half-life of O^{14} has also been measured by these authors who find $T_{1/2} = (71.00 \pm 0.13)$ sec.

In view of the divergence between the various values reported for the branching and because of the fact that in all of the preceding experiments the O^{14} activity was made by the $N^{14}(p, n)O^{14}$ reaction, we thought it would be interesting to restudy the properties of O^{14} . In our experiments we formed O^{14} by the reaction $C^{12}(He^3, n)O^{14}$ and we detected the positrons by means of an intermediate-image focusing spectrometer.

Ne¹⁸

The isotope Ne¹⁸ was first observed and studied by Gow and Alvarez¹⁰ using the reaction $F^{19}(p, 2n)Ne^{18}$. These authors measured the half-life of Ne¹⁸ as $T_{1/2} = (1.6 \pm 0.2)$ sec and by means of a 180° magnetic spectrograph they found a single β^+ branch of maximum energy (3.2 ± 0.2) MeV. They attributed this branch to the positron decay of Ne¹⁸ to the ground state of F¹⁸.

It is only recently that new measurement have been carried out by Eccleshall and Yates¹¹ on the decay of Ne¹⁸ in order to study possible branches to excited states of F¹⁸. The method consisted of bombarding a quartz target with He³ ions of 5.2 MeV and measuring the delayed gamma-ray spectra following the reaction $O^{16}(He^3, n)Ne^{18}$. These authors found a gamma-ray transition of (1.035 ± 0.010) MeV and showed that its intensity decreased with a half-life $T_{1/2} = (1.7 \pm 0.4)$ sec. They concluded that this gamma radiation corresponds to a transition from the 1.04-MeV level in F¹⁸ which is fed by the positron decay of Ne¹⁸. This same result was confirmed later by Butler and Dunning,¹² who in preliminary work¹³ had first indicated that Ne¹⁸ decays

by positron emission to the 1.04 and 1.70-MeV level of F¹⁸. These authors also measured the half-life of Ne¹⁸ by observing the annihilation radiation due to positrons in the disintegration of Ne¹⁸ and found $T_{1/2} = (1.46 \pm 0.07)$ sec. Moreover, by a comparison of the intensity of the photopeaks of the annihilation radiation and of the gamma radiation of 1.04 MeV, Butler and Dunning measured the relative branching as $(7 \pm 2)\%$ to the level at 1.04 MeV and $(93 \pm 2)\%$ to the ground state. In other papers^{14,18} the same authors measured the threshold energy for the $O^{16}(He^3, n)Ne^{18}$ reaction to be (3.811 ± 0.015) MeV, a value from which they calculated the end point for positrons populating the ground state of F¹⁸ to be (3.423 ± 0.013) MeV. Later, many authors¹⁵⁻¹⁸ made determinations of the ground-state Q value of the $O^{16}(He^3, n)Ne^{18}$ reaction from which it was possible to calculate the value of the end point of the positron transition to the ground state of F¹⁸ as being (3.423 ± 0.020) MeV. Some of these experiments were carried out to determine which of the four levels of F¹⁸, situated in the region of excitation of 1 MeV, was the 0^+ , $T=1$ level analogous to the ground states of Ne¹⁸ and O¹⁸.

Our experiments consisted of measurements of the positron spectrum with better precision than in previous work as well as a determination of the half-life of Ne¹⁸ by observations on the positrons.

Si²⁶

It was Tyren and Tove¹⁹ who, by using the reaction $Al^{27}(p, 2n)Si^{26}$, first obtained evidence for an activity of half-life $T_{1/2} = 1.7$ sec which they attributed to the isotope Si²⁶. Later, Ajzenberg-Selove and Dunning^{15,16} showed that Si²⁶ ought to have a positron activity based on measurements of the Q value of the $Mg^{24}(He^3, n)Si^{26}$ reaction from the results of which they deduced that the mass difference $Si^{26} - Al^{26}$ is (5.05 ± 0.08) MeV.

A similar study of the radioactivity of Si²⁶ was made by Robinson and Johnson²⁰ who also used the reaction $Mg^{24}(He^3, n)Si^{26}$. In their work Si²⁶ was produced by an He³ beam from a cyclotron and the sample was transported to a NaI(Tl) detector by a pneumatic transfer system (transit time of 0.25 sec). Measurements of the decay, which were carried out on the photopeak of annihilation radiation as well as on that part of the gamma-ray spectrum situated below discrimination levels of 2.8, 3.8, and 4 MeV, showed

⁶ K. Ott, Z. Naturforsch. **14a**, 769 (1959).

⁷ R. K. Bardin, C. A. Barnes, W. A. Fowler, and P. A. Seeger, Phys. Rev. **127**, 583 (1962).

⁸ H. A. Weidenmuller, Phys. Rev. **127**, 537 (1962).

⁹ R. J. Blin-Stoyle and J. Le Tourneux, Ann. Phys. (N. Y.) **18**, 12 (1962).

¹⁰ J. D. Gow and L. W. Alvarez, Phys. Rev. **94**, 365 (1954).

¹¹ D. Eccleshall and M. J. L. Yates, Proc. Phys. Soc. (London) **77**, 93 (1961).

¹² J. W. Butler and K. L. Dunning, Phys. Rev. **121**, 1782 (1961).

¹³ J. W. Butler and K. L. Dunning, Bull. Am. Phys. Soc. **5**, 101 (1960).

¹⁴ K. L. Dunning and J. W. Butler, Bull. Am. Phys. Soc. **4**, 444 (1959).

¹⁵ F. Ajzenberg-Selove and K. L. Dunning, Bull. Am. Phys. Soc. **5**, 36 (1960).

¹⁶ F. Ajzenberg-Selove and K. L. Dunning, Phys. Rev. **119**, 1681 (1960).

¹⁷ J. H. Towle and B. E. F. Macefield, Proc. Phys. Soc. (London) **77**, 399 (1961).

¹⁸ K. L. Dunning and J. W. Butler, Phys. Rev. **123**, 1321 (1961).

¹⁹ H. Tyren and P. A. Tove, Phys. Rev. **96**, 773 (1954).

²⁰ E. L. Robinson and O. E. Johnson, Phys. Rev. **120**, 1321 (1960).

evidence for an activity (2.1 ± 0.3) sec which is assigned to Si^{26} . These measurements showed that the end-point energy of the positrons emitted by Si^{26} is greater than 3.5 MeV. The same authors showed that the intensity of a gamma-ray line of (824 ± 15) keV which appears in the spectrum decays with a half-life of less than 90 sec. They assigned this gamma radiation to a transition from the 1.059-MeV level to the isomeric level of 0.229 MeV in Al^{26} and thus established a decay scheme of Si^{26} to Al^{26} taking place in two branches of 3.76 and 2.94-MeV energy. Since no direct measurement of the positron activity of Si^{26} had been made, we undertook such a measurement in order to determine the maximum energies of the various positron branches as well as the branching ratios.

S^{30}

A theoretical study of Coulomb energies in the light nuclei made by Peaslee²¹ showed that the 0^+ , $T=1$ ground state of S^{30} should occur about 5.4 MeV below the 0^+ , $T=1$ state of P^{30} . This suggested that S^{30} should decay by positron emission to P^{30} . The first measurements giving evidence for the radioactivity of S^{30} were made simultaneously by Johnson *et al.*²² and by Robinson *et al.*²³ using the reaction $Si^{28}(He^3, n)S^{30}$. These two groups of authors found half-lives for S^{30} of (1.5 ± 0.1) sec and (1.35 ± 0.1) sec, respectively. They found a positron branch of maximum energy 4.3 MeV in coincidence with a gamma ray of 0.676 MeV. Robinson *et al.*²³ furthermore observed positrons of about 5-MeV energy which they assigned to a branch going to the ground state of P^{30} . Our experiments constitute the first measurements of the positron decay of S^{30} and its branching ratios by means of a magnetic spectrometer. We also measured the mean life of S^{30} by detecting positrons of selected energy and observed the gamma-ray spectrum in coincidence with positrons.

EXPERIMENTAL METHODS

The isotopes which we studied were produced by reactions induced by the He^3 beam from a 5.5-MeV Van de Graaff accelerator. After analysis by a 90° deflection magnet the beam was monoenergetic to 0.4%. In the vicinity of the magnet a beam chopper was installed which rotated at 1350 rpm. Thus, the beam passed through the chopper during 22 msec and was interrupted during the remainder of the time. This apparatus triggered an electronic gate in such a way that the detecting circuit registered counts only during the period between bombardments. After the beam passed through the chopper it went through quadrupole magnets which refocused the beam on the target. These lenses were situated 3 m from the target and were not

affected by the magnetic field of the spectrometer. An aperture 2 mm in diameter placed just in front of the target insured that the target was always bombarded in the same spot.

Before beginning any measurements the target was bombarded for a time (sometimes several hours) equal to several half-lives of the isotope being produced that had the longest half-life. Thus, for the conditions in which the beam intensity was constant, secular equilibrium was attained in the target corresponding to a source of infinite half-life. Preliminary measurements were made to test whether or not we had achieved this equilibrium. A Faraday cup placed beyond the target was attached electrically to the target. The charge collected on this system was measured by a current integrator which served to normalize the number of counts. A clock measured the integration time and indicated whether or not the beam was constant from one measurement to another. In general we used only those measurements in which the variation in the beam intensity did not exceed 5%.

In study of the isotope O^{14} we bombarded targets of self-supporting carbon, 8 mg/cm² in thickness. These targets, which were made from a suspension of graphite in alcohol (Alcool-dag), withstood a beam current of about 0.5 μ A. For the study of Ne^{18} , which was produced in the reaction $O^{16}(He^3, n)Ne^{18}$, we used in the beginning of our experiments targets consisting of a deposit of titanium oxide, 5–10 mg/cm² thick on a nickel foil. After bombardment times of the order of 1–2 h, these targets disintegrated. Later we used targets of tantalum oxide, 10 mg/cm² in thickness. These targets remained stable under bombardment during the entire length of the experiments. Foils of natural magnesium of 5 mg/cm² thickness were used for production of the isotope Si^{26} in the reaction $Mg^{24}(He^3, n)Si^{26}$. In the discussion of our results we shall mention the reactions produced in Mg^{25} (10.1%) and Mg^{26} (11.2%) which are present in natural magnesium. For the experiments on S^{30} we used the reaction $Si^{28}(He^3, n)S^{30}$. The target consisted of a deposit of natural silicon on nickel foil 0.2 mg/cm² in thickness. Natural silicon contains 92.2% Si^{28} , 4.7% Si^{29} , and 3.1% Si^{30} . We shall also discuss the Si^{29} and Si^{30} reactions later.

The major part of our work was carried out with the help of a Siegbahn-Slätis intermediate-image focusing spectrometer. The activity to be studied was produced in the target located at the normal source position of the spectrometer. This spectrometer can focus electrons having energies up to 7 MeV. In all of our experiments it was adjusted for a transmission of 5% of 4π corresponding to a resolution of 4%. The electrons selected by the spectrometer were focused onto a bell-type Geiger-Müller counter whose window stopped all electrons having energies lower than 100 keV. Only positrons could reach the detector because the negative electrons were stopped by a spiral baffle mounted inside the spectrometer. A calibration was made before and

²¹ D. C. Peaslee, Phys. Rev. **95**, 717 (1954).

²² R. G. Johnson, L. F. Chase, and W. L. Imhof, Bull. Am. Phys. Soc. **5**, 406 (1960).

²³ E. L. Robinson, J. I. Rhode, and O. E. Johnson, Phys. Rev. **122**, 879 (1961).

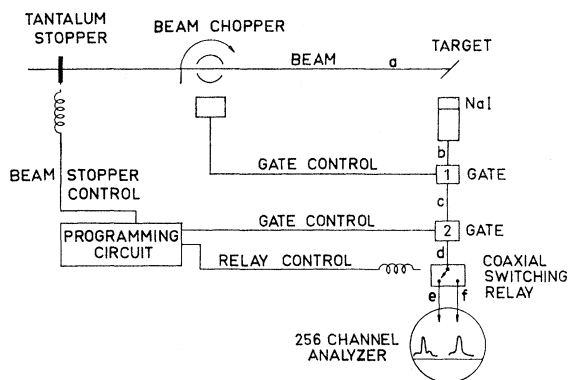


Fig. 1. Schematic diagram of the circuit programmer.

after each series of measurements by using the 976-keV internal conversion line from a source of Bi^{207} . By means of a source of thorium ($B+C+C''$) we checked that the linearity of the instrument was good to 0.1% up to 3 MeV. We furthermore verified that the stability of the current producing the field was good to $\pm 0.2\%$. These figures agree with specifications given by the manufacturer of the spectrometer (LKB Products Company, Stockholm, Sweden). The position of the source was reproducible to about 0.1 mm.

In another part of our work we used scintillation detectors to study the delayed gamma and beta-ray spectra from the same targets which served for the measurements in the magnetic spectrometer. For this type of measurement the targets were placed outside the spectrometer. In the detection of gamma rays, we used a $1\frac{1}{2} \times 1\frac{1}{2}$ -in. sodium iodide crystal mounted on a Radiotechnique 153 AVP photomultiplier tube. This detector had a resolution of 8% for the 661-keV gamma ray of Cs^{137} . The electronic gate produced by the beam

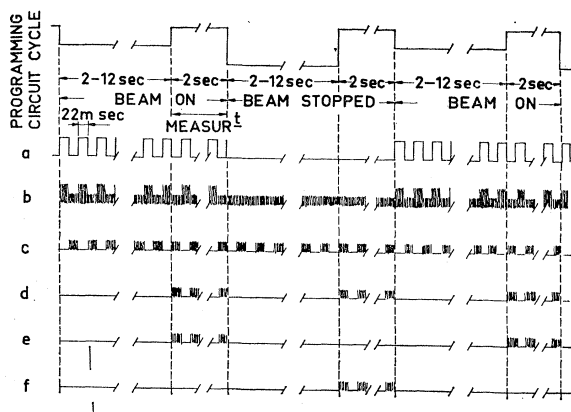


FIG. 2. This figure represents the oscilloscope images observed at different parts of the circuit. In (a) one first sees the intensity of the chopped beam and then interrupted by the tantalum shutter. (b) Shows the pulses from the detector; they are numerous and large when the target is being bombarded but are small and less numerous when the beam is cut off. In (c), (d), (e), and (f) one sees the effect of the gate and of the switching relay.

chopper allowed the counting of only the delayed gamma rays. The pulse-height spectrum suffers no amplitude distortion because of the gate. We have checked this by measurements on the Na^{22} gamma-ray spectrum. The nonlinearity, less than one channel in a 256-channel analyzer, is thus less than 0.5% for the 1.28-MeV gamma-ray line. For the detection of the spectra of delayed electrons the same principle was used except that the sodium iodide crystal was replaced by a Ne 102 plastic scintillator 1 cm in thickness.

In the course of the measurements of the gamma-ray spectra with the arrangement described above we were able to see, in addition to the very intense 510-keV line, one or more weak gamma-ray lines associated with positron activities. However, it was difficult to attribute these gamma rays to a particular isotope. In order to do so we constructed a circuit programmer with which we were able to make an estimate of the half-life of the associated radioactivity.

The essential idea of this arrangement (Figs. 1 and 2) was the following: We compared two measurements, the first consisting of counts from a spectrum delayed

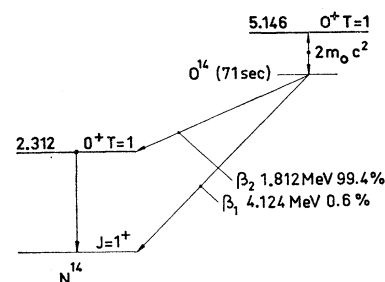


FIG. 3. Decay scheme of O^{14} .

for only a short time beginning just after the beam was cut off. Some seconds later a second measurement of the spectrum was made for a time equal to the first measurement.

The system was arranged as follows: After radioactive equilibrium of the source was achieved the photomultiplier pulses were passed for a period of 2 sec through the electronic gate actuated by the beam chopper, to the left-hand part (channels 1 to 128) of a 256-channel pulse-height analyzer. We therefore recorded the spectrum due to gamma rays associated with beta activities for a target in radioactive equilibrium. After this measurement the beam was cut completely by a tantalum shutter, but the beam chopper continued to turn. At that moment, the activity in the target began to decay. After a time adjustable from 2- to 12-sec pulses were recorded in the right-hand part (channels 129-256) of the analyzer. In the course of this measurement, which also lasted 2 sec, the spectrum recorded was that due to a source after decay for a known time from 2 to 12 sec. Since the beam chopper and the electronic gate continued to operate the net counting time was the same for the two meas-

TABLE I. Reactions due to the bombardment of a carbon target by He³ ions.^a

Abundance			Half-life	E_{\max} (MeV)	Q (MeV)	Remarks
98.89%	C ¹² (He ³ , α)C ¹¹	β^+	20.44 \pm 0.04 min	0.968 \pm 0.008	1.856	yes
	C ¹² (He ³ , β)N ¹²	β^+	11.43 \pm 0.05 msec	16.37 \pm 0.06	-17.48	no
	C ¹² (He ³ , d)N ¹³	β^+	9.96 \pm 0.03 min	1.190 \pm 0.003	-3.553	no
	C ¹² (He ³ , p)N ¹⁴	stable			4.772	no
	C ¹² (He ³ , n)O ¹⁴	β^+	71.00 \pm 0.13 sec	4.124 \pm 0.002 1.812 \pm 0.014	-1.148	yes our study
1.11%	C ¹³ (He ³ , α)C ¹²	stable			15.63	no
	C ¹³ (He ³ , β)N ¹³	β^+	9.96 \pm 0.03 min	1.190 \pm 0.003	-2.240	yes
	C ¹³ (He ³ , d)N ¹⁴	stable			2.052	no
	C ¹³ (He ³ , p)N ¹⁵	stable			10.67	no
	C ¹³ (He ³ , n)O ¹⁵	β^+	123.6 \pm 0.5 sec	1.733 \pm 0.005	7.126	yes

^a All of this information was taken from F. Ajzenberg-Selove and T. Lauritsen (Ref. 1) except for O¹⁴ (Ref. 7). The remarks "no" indicate that this reaction does not produce positron activities at the bombarding energy of 3.8 MeV. The remarks "yes" indicate that such isotopes ought to be produced and we should take them into account in the interpretation of our experiments.

urements. Immediately after this second measurement the programming circuit put the beam back on the target. After a time equal to that during which the beam had been cut off in the course of the preceding operation (2 to 12 sec) a time necessary for the reactivation of the target, a new recording of 2-sec duration was carried out on the left-hand part of the analyzer and this cycle of operations was started again. The fact that the two measurements were carried out only a few seconds apart made the results nearly independent of beam current fluctuations or the deterioration of the target. Complete measurements lasted between a half-hour and one hour. In the course of these measurements we observed that the intensities of the 510-keV line in the two spectra differed only a small amount. This indicated that the main part of the radioactivity producing this line decayed with half-lives considerably longer than the time during which the beam was cut off over the range adjustable by the programmer. On the other hand, the various other gamma-ray lines seen in the spectra from the target in radioactive equilibrium were diminished in intensity or even disappeared in the spectrum measured after cutting off the beam. The comparison of the intensities of these lines allowed an estimate to be made of the half-life of the decay of the corresponding radioactivity and allowed us to identify unambiguously a given isotope.

The half-life of the source was measured after cutting off the beam by observing the pulses from the spectrometer detector. Our procedure was to measure the decay of selected parts of the spectrum in the spectrometer. Thus, if the current in the spectrometer was adjusted to a value corresponding to an energy E , the counter pulses corresponded to positrons of energy $E(1\pm 0.02)$ MeV. For these measurements we used an RCL 128 channel analyzer operating as a time analyzer. This device registered pulses in a given channel only during a predetermined time interval after which they were fed to the next channel, and so forth. Thus the equipment recorded directly the decay curve of the source. In the cases of very low statistics we made

successive measurements and added the curves together. In between two measurements the source was reactivated.

EXPERIMENTAL RESULTS

O¹⁴

The isotope O¹⁴ was produced in the reaction C¹²(He³, n)O¹⁴ by bombarding a target of natural carbon with He³ ions of 3.8-MeV energy. Natural carbon contains 99% C¹² and 1% C¹³ and the reactions given in Table I are the main ones possible. Thus, we should expect to produce, aside from the isotope O¹⁴ in which we are interested, the isotopes C¹¹ and N¹³. In the event of an oxygen contamination we also should produce O¹⁵ and F¹⁸.

The measured spectra (Fig. 4) shows three groups of considerably different intensities. A first group having a maximum energy of about 1 MeV corresponds to the positron spectrum of C¹¹. The second group of maximum energy 1.8 MeV can be attributed to positrons due to

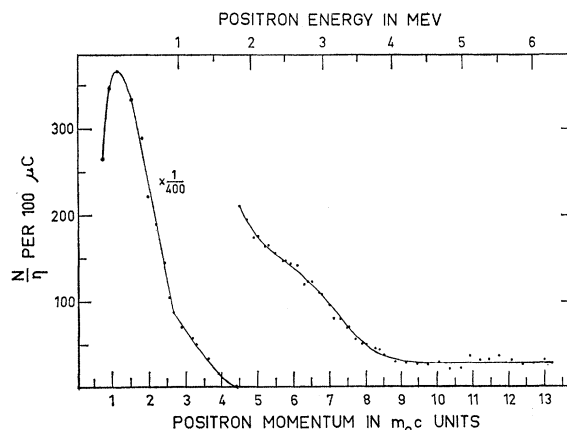


FIG. 4. Spectrum of positrons following the bombardment of a carbon target by He³ ions. ($E_b = 3.8$ MeV with a beam intensity of $0.3 \mu\text{A}$). Components of the spectrum due to C¹¹ (0.97 MeV) and to O¹⁴ (1.81 MeV and 4.1 MeV) can be distinguished.

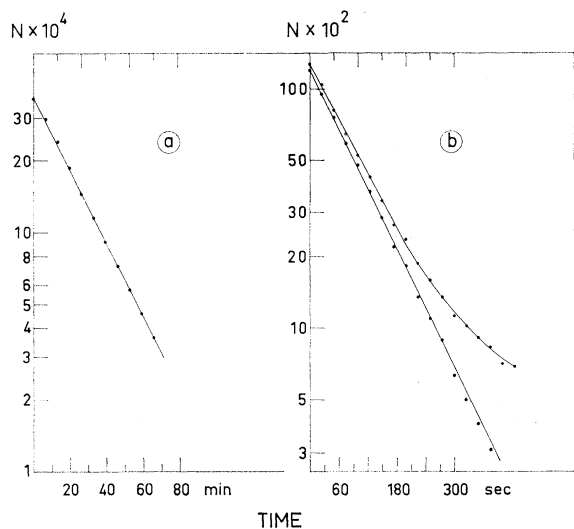


FIG. 5. (a) Half-life of C^{11} determined from the decay of positrons of 580 keV selected by the spectrometer; $T_{1/2} = (20.3 \pm 0.3)$ min. (b) Half-life of O^{14} determined from the decay of positrons at a focusing energy of 2.7 MeV. The upper curve represents the total yield and the lower curve is obtained after subtraction of the background; $T_{1/2} = (71.3 \pm 0.1)$ sec.

the decay of O^{14} to the 2.3-MeV first excited state of N^{14} . A third group having a maximum energy greater than 1.8 MeV had a very low intensity and *a priori* was thought to be the result of a positron transition of O^{14} to the ground state of N^{14} .

In order to better identify the different parts of the spectrum we made measurements on the decay of the beta-ray activity in different parts of the spectrum by using the method described in the preceding section. Altogether a dozen measurements were made. We thus

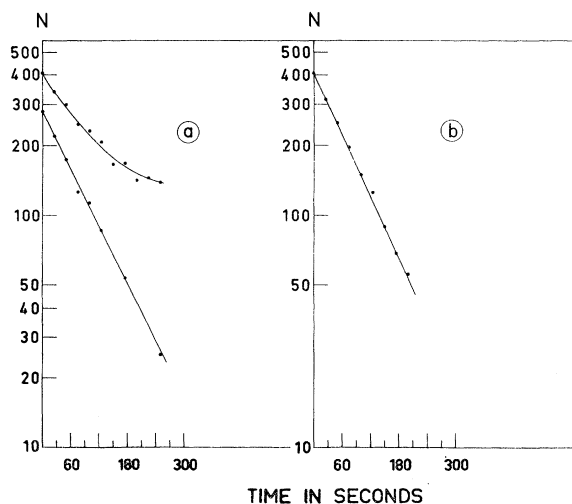


FIG. 6. (a) Half-life of O^{14} determined from the decay of positrons at a focusing energy of 2.6 MeV. The upper curve represents the sum of 10 individual measurements. The lower curve is obtained after the subtraction of the background; $T_{1/2} = (73 \pm 5)$ sec. (b) Half-life of O^{14} determined from the decay of the 2.3-MeV gamma rays; $T_{1/2} = 72$ sec.

found $T_{1/2} = (20.3 \pm 0.2)$ min at 580 keV [Fig. 5(a)]. This value corresponds to those reported¹ by other authors for the half-life of C^{11} . In the second part of the spectrum for positrons of 0.97 MeV our result $T_{1/2} = (71.3 \pm 0.1)$ sec [Fig. 5(b)] is to be compared with (71.0 ± 0.1) sec reported by Bardin *et al.*⁷ for the half-life of O^{14} . Other measurements made between 0.97 and 1.8 MeV confirmed this value. For that part of the spectrum of very low intensity we found $T_{1/2} = (73 \pm 5)$ sec for positrons of 2.6 MeV [Fig. 6(a) and $T_{1/2} = (63 \pm 10)$ sec for positrons of 3 MeV. We thus assigned this branch also to the decay of O^{14} . If other isotopes such as N^{18} , O^{18} , and F^{18} were present in appreciable amounts, the measurements of the half-lives in different parts of the spectrum would have given results different from the known half-lives of C^{11} and O^{14} . The fact that such differences of the half-lives

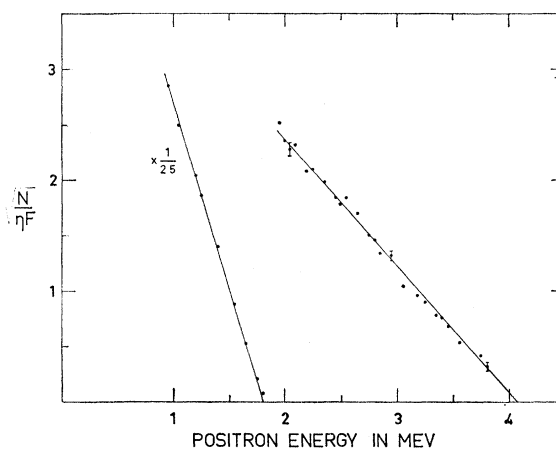


FIG. 7. Kurie-plot analysis of the O^{14} positron spectrum. The maximum energies are $E_1 = 4.085 \pm 0.030$ MeV and $E_2 = 1.821 \pm 0.007$ MeV.

were not observed allows us to conclude that in this experiment we produced only C^{11} and O^{14} in appreciable quantities. However the delayed gamma-ray spectrum showed a line of energy 2.3 MeV. The decay of this line corresponds to a half-life of 72 sec [Fig. 6(b)]. We therefore assign this to the decay of the first excited state of N^{14} as fed by the positron decay of O^{14} .

Following these preliminary experiments we concentrated our efforts on the precision measurements of the spectra of positrons emitted by O^{14} . In order to check for any variations of yield, due to a deterioration of the target for example, we measured at regular intervals a series of points in that part of the intense spectrum between 1 and 1.8 MeV. Between the first and second series of these check measurements, we also recorded the positron intensities at 20 different field settings between 1.8 and 6.5 MeV. Between the second and third check runs we also measured a new series of 20 points just as in the first set of measurements and again for those beta-ray energies over the range 1.8 to 6.5

TABLE II. Experimental results on the radioactivity of O¹⁴.

	Gerhart ^a -Sherr ^b	Bardin ^c	Our measurements
E_1	...	4.124 ± 0.002 MeV	4.085 ± 0.030 MeV
E_2	1.835 ± 0.008 MeV	1.8120 ± 0.0014 MeV	1.821 ± 0.007 MeV
Branching ratio			
Branch 1	(0.6 ± 0.1)%	...	(0.65 ± 0.05)%
Branch 2	(99.4 ± 0.1)%	...	(99.35 ± 0.05)%
f_1	(2.0 ± 0.3) 10 ⁷	...	(1.7 ± 0.2) 10 ⁷
log f_1	7.30 ± 0.07	...	7.23 ± 0.04
f_2	3275 ± 75	3075 ± 10	3137 ± 70
log f_2	3.515 ± 0.010	3.488 ± 0.002	3.496 ± 0.010
Half-life	72.1 ± 0.4 sec	71.00 ± 0.13 sec	71.3 ± 0.1 sec

^a See Ref. 4.

^b See Ref. 2.

^c The results of Bardin (Ref. 7) were determined by using the Q values for the reactions C¹²(He³, n)O¹⁴ and C¹²(He³, p)N¹⁴. See also Refs. d-g below, the results of which are not reported in this table.

^d J. R. Penning and F. H. Schmitt, Phys. Rev. **94**, 779A (1954).

^e D. A. Bromley, E. Almquist, H. E. Gove, A. E. Litherland, E. B. Paul, and A. J. Ferguson, Phys. Rev. **105**, 957 (1957).

^f J. W. Butler and R. O. Bondelid, Phys. Rev. **121**, 1770 (1961).

^g D. L. Hendrie and J. B. Gerhart, Phys. Rev. **121**, 846 (1961).

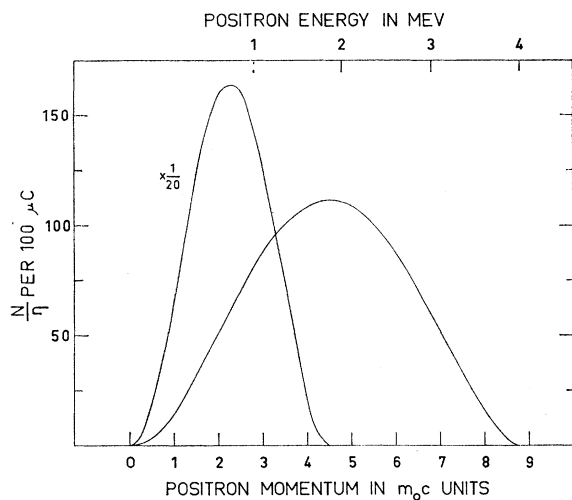


FIG. 8. Determination of the O¹⁴ positron branching ratios; $r_1 = (0.65 \pm 0.05)\%$ and $r_2 = (99.35 \pm 0.05)\%$.

MeV. The field settings of each of these series were divided in such a way that after 4 passes over the low intensity part of the spectrum each of these points was measured two times.

We required that each set of 20 points that were bracketed by two check measurements were identical with each other within $\pm 5\%$. The results of each series were normalized according to the ratio of the intensities of the check points. The sum of 12 such normalized series were used for the determination of maximum energies and for the branching ratios. The maximum energies calculated by the method of least squares are $E_1 = (4.085 \pm 0.030)$ MeV and $E_2 = (1.821 \pm 0.007)$ MeV.

By making Kurie plots (Fig. 7) we were able to reconstruct the spectrum belonging to each transition and to calculate the branching ratios (Fig. 8). Table II shows that our results are in agreement with those of Sherr *et al.*⁵ In particular we find $(0.65 \pm 0.05)\%$ for the relative branching ratio of the 4.1 MeV branch to the ground state.

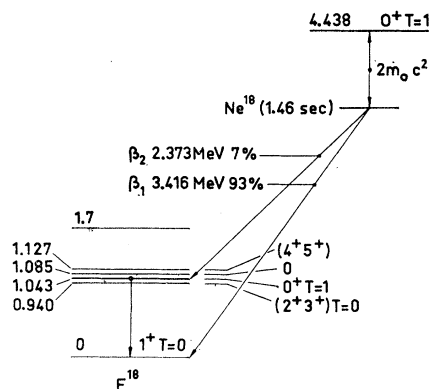


FIG. 9. Decay scheme of Ne¹⁸.

Ne¹⁸

The isotope Ne¹⁸ was produced by the reaction O¹⁶(He³, n)Ne¹⁸ at the resonance $E_{He^3} = 5.2$ MeV. Evidently we could also expect to produce isotopes resulting from other reactions on O¹⁶. Since the target was prepared using natural oxygen we should also expect to produce isotopes from the bombardment of He³ on O¹⁷ (0.037%) and O¹⁸ (0.204%). All the possible reactions are given in Table III. Moreover, we noticed that during the experiments the targets accumulated carbon deposits in the region where they were struck by the beam giving rise to the isotopes C¹¹ and O¹⁴ which we have already discussed (see Table I). Only the isotopes O¹⁵, F¹⁸, F¹⁷, and Ne¹⁹ could, in principle, be produced in the target aside from the Ne¹⁸ which we wished to study.

In the measured spectra we saw three groups of considerably different intensities (Fig. 10). The first

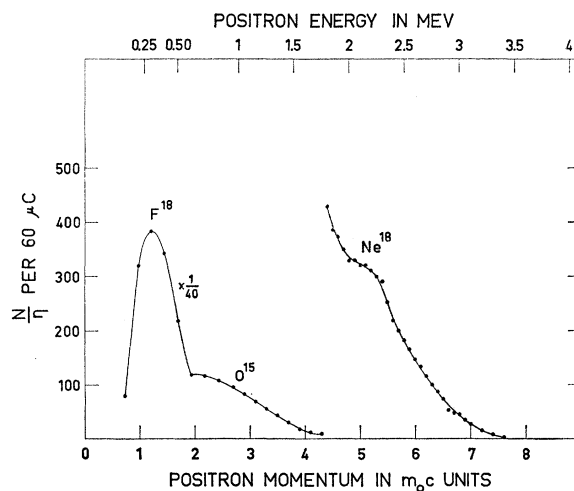


FIG. 10. The spectrum of positrons following the bombardment of an oxygen target by He³ ions ($E_b = 5.2$ MeV with a beam intensity of 0.5 μ A). The components of the spectrum belonging to F¹⁸ (0.65 MeV), O¹⁵ (1.73 MeV) and Ne¹⁸ (3.42 MeV) are indicated.

TABLE III. Reactions due to the bombardment of an oxygen target by He³ ions.^a

			Half-life	E_{\max} MeV	Q	Remarks
99.759%	$O^{16}(He^3, \alpha)O^{15}$	β^+	123.6 \pm 0.5 sec	1.733 \pm 0.005	4.923	yes
	$O^{16}(He^3, t)F^{16}$	proton unstable	-15.61	no
	$O^{16}(He^3, d)F^{17}$	β^+	66.0 \pm 0.3 sec	1.748 \pm 0.006	-4.898	no
	$O^{16}(He^3, p)F^{18}$	β^+	111 \pm 1 min	0.649 \pm 0.009	2.045	yes
	$O^{16}(He^3, n)Ne^{18}$	β^+	1.46 \pm 0.07 sec	3.423 \pm 0.012	2.380 \pm 0.013	yes our study
0.037%	$O^{17}(He^3, \alpha)O^{16}$	stable	16.43	no
	$O^{17}(He^3, t)F^{17}$	β^+	66.0 \pm 0.3 sec	1.748 \pm 0.006	-2.78	yes
	$O^{17}(He^3, d)F^{18}$	β^+	111 \pm 1 min	0.649 \pm 0.009	0.125	yes
	$O^{17}(He^3, p)F^{19}$	stable	8.313	no
	$O^{17}(He^3, n)Ne^{19}$	β^+	17.4 \pm 0.2 sec	2.24 \pm 0.01	4.274	yes
0.204%	$O^{18}(He^3, \alpha)O^{17}$	stable	12.50	no
	$O^{18}(He^3, t)F^{18}$	β^+	111 \pm 1 min	0.649 \pm 0.009	-1.685	yes
	$O^{18}(He^3, d)F^{19}$	stable	2.470	no
	$O^{18}(He^3, p)F^{20}$	β^-	11.4 sec	5.413 \pm 0.013	6.850	no
	$O^{18}(He^3, n)Ne^{20}$	stable	13.11	no

^a All this information was taken from F. Ajzenberg-Selove and T. Lauritsen (Ref. 1) except for Ne¹⁸ (Ref. 12). The remark "no" signifies that this reaction did not produce positron activity at the bombarding energy of 5.2 MeV. The remark "yes" indicates that such isotopes ought to be produced and that we should take them into account in the interpretation of our results.

part, having a maximum energy of about 0.6 MeV, corresponds to the activity F¹⁸. The second component, which ends at about 1.7 MeV, can be attributed principally to positrons from the decay of O¹⁵. Finally, a third much less intense part whose maximum energy lies at about 3 MeV should be the spectrum of positrons emitted by Ne¹⁸.

Just as in the study of O¹⁴ we measured the half-life at several positron energies in order to identify the isotopes produced in the target. Thus, in the region of energies above 1.8 MeV, six measurements made at positron energies of 2.15, 2.3, 2.35, 2.5, 2.64, and 2.95 MeV gave results compatible with each other. The average of these results is $T_{1/2} = (1.47 \pm 0.10)$ sec. This value compares with the Ne¹⁸ half-life (1.46 \pm 0.07) sec measured by Butler and Dunning¹² and consequently we assign this branch to the decay of Ne¹⁸. In the

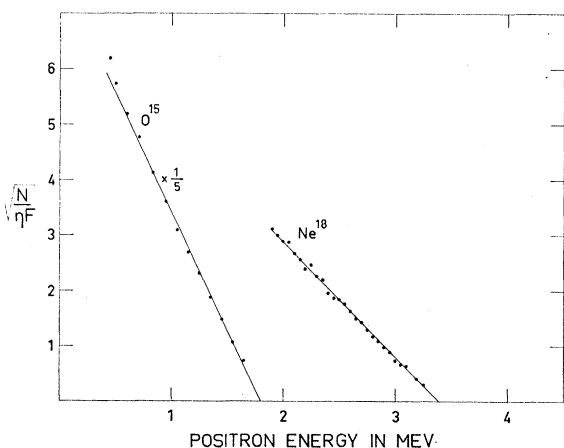


FIG. 11. Kurie-plot analysis of the positron spectrum following the He³ bombardment of an oxygen target. The end-point energy of the Ne¹⁸ component is (3.416 \pm 0.009) MeV.

portion of the spectrum ending at about 1.7 MeV we obtained $T_{1/2} = 130$ sec for the positrons of 1 MeV, $T_{1/2} = 106$ sec at 1.70 MeV and $T_{1/2} = 60$ sec at 1.75 MeV. Finally for positrons of 1.8 MeV the activity having a half-life of about 1 min had disappeared completely and there remained only a rapid decay of the order of seconds corresponding to Ne¹⁸. We conclude that in the portion of the spectrum between 1 and 1.8 MeV we were seeing a mixture of two isotopes the most abundant of which has a half-life of about 130 sec and the other a half-life of about 60 sec. Also we were able to say that the maximum energy corresponding to the isotope of 130 sec occurs between 1.7 and 1.75 MeV and that the spectrum of the other isotope (60 sec) ought to have a maximum energy greater than 1.75 MeV. In examining the various possible reactions we therefore see that we have a mixture consisting of O¹⁵ reported with $T_{1/2} = 123$ sec and $E_{\max} = 1.75$ MeV and a weak component of O¹⁴ reported to have $T_{1/2} = 71$ sec and $E_{\max} = 1.82$ MeV. The presence of F¹⁷ and Ne¹⁹ is not completely excluded but these activities are not produced in appreciable quantities. In the portion of the spectrum of energy lower than 0.6 MeV we have measured a decay which is a composite of two half-lives of 20 min and 111 min. These two values correspond with those reported for C¹¹ and F¹⁸.

This spectrum whose various parts have been identified make it difficult to carry out a complete study of the decay of Ne¹⁸. However, Butler¹² reports that Ne¹⁸ decays in two branches, one of 3.4 MeV with a relative intensity of 93% and the other of 2.3 MeV with a branch of 7% intensity. Although we were able to make good observations on the energetic branch most of the inner branch is masked by the activities whose energies are less than 1.8 MeV and we have not been able to study Ne¹⁸ in this region with the magnetic spectrometer.

We made nine accurate measurements of the complete spectrum. The Kurie plot for that portion of the spectrum associated with Ne¹⁸ is linear within the statistical errors (Fig. 11). This plot has the characteristic shape of an allowed transition. The calculation of the maximum energy by the method of least squares is $E_1 = (3.416 \pm 0.009)$ MeV, a result which takes into account the energy lost by the electrons in passing through the target (15 to 20 keV according to the target being used). The Kurie plot for the portion of the spectrum between 1 and 2 MeV is straight and has a maximum energy of (1.790 ± 0.010) MeV. This value lies between those reported for O¹⁵ (1.733 MeV) and O¹⁴ (1.820 MeV) and confirms that we have a mixture of two isotopes.

Because of the reasons indicated above, we have not been able to observe the second branch of positrons in the decay of Ne¹⁸ using the magnetic spectrometer. We have, nevertheless, been able to confirm that the second branch corresponds to a gamma-ray line having an energy of (1.030 ± 0.020) MeV. By using the circuit programmer described previously and taking into account the effect of pile-up of the 0.511-MeV gamma rays, we find that the gamma-ray line decays with a half-life of about 1.5 sec (Fig. 12).

Ne¹⁸ being the only isotope present with a half-life of this order of magnitude we identify the gamma-ray line as being associated with the decay of the 1.04-MeV level in F¹⁸ fed by a positron branch of Ne¹⁸. We therefore confirm that Ne¹⁸ decays in two branches, a result in agreement with those established by other authors.^{11,12}

In order to establish the branching ratios of these two beta-ray transitions, we measured by means of a scintillation detector the delayed positron spectra which we then compared with the delayed gamma-ray spectra recorded for the same amount of charge collected on the target. If we call $N_{0\gamma}$ the total number of gamma rays of 1 MeV emitted by the target and $N_{0\beta}$ the total number of positrons of the 3.4-MeV branch emitted for the same integrated charge, the branching ratios can be written in the form,

$$r_1 = N_{0\beta} / N_{0\gamma} + N_{0\beta} \quad \text{and} \quad r_2 = N_{0\gamma} / N_{0\gamma} + N_{0\beta}$$

$N_{0\gamma}$ calculated from N_γ the number of pulses in the photopeak of 1 MeV (corrected for pile-up) is given by

$$N_{0\gamma} = N_\gamma / \epsilon_\gamma \Omega_\gamma,$$

where Ω_γ is equal to the solid angle of the gamma-ray detector and ϵ_γ is the detection efficiency for a gamma ray of 1 MeV in the photopeak. In an analogous manner,

$$N_\beta = N_\beta / a_\beta \Omega_\beta \epsilon_\beta,$$

where N_β is the number of electrons detected that have energies between 2.3 and 3.4 MeV, Ω_β is the solid angle of the detector, ϵ_β is the efficiency for detecting β rays (≈ 1) and a_β is the fraction of electrons of energy lying

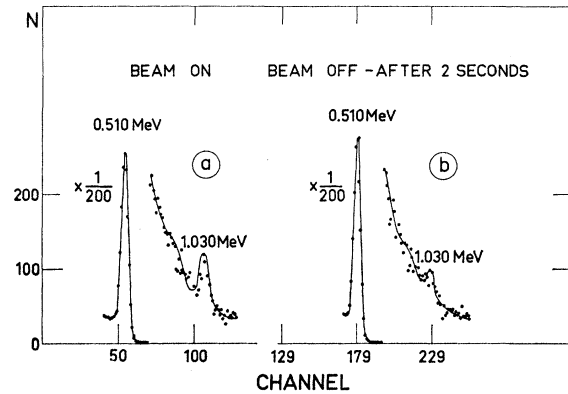


FIG. 12. Gamma-ray spectra from the oxygen target following He³ bombardment. Curve (a) shows the spectrum observed by means of a circuit programmer when the source is in radioactive equilibrium. In addition to the intense 0.510-MeV line, a line is seen at 1.030 ± 0.020 MeV. Curve (b) shows the same spectrum after the beam has been cut off for two seconds. The line at 1.030 MeV has diminished in intensity and is assigned to the decay of a level of F¹⁸ fed in the β^+ radioactivity of Ne¹⁸.

between 2.3 and 3.4 MeV. By using these relationships, one can calculate

$$r_2 = \frac{N_{0\gamma}}{N_{0\gamma} + N_{0\beta}} = \frac{1}{1 + \frac{N_{0\beta}}{N_{0\gamma}}} = \frac{1}{1 + \frac{N_\beta}{N_\gamma} \frac{1}{a_\beta} \frac{\epsilon_\gamma \Omega_\gamma}{\epsilon_\beta \Omega_\beta}};$$

N_β and N_γ are deduced directly from the measurements; a_β has a magnitude that is easy to determine from the electron spectrum observed in the magnetic spectrometer. The ratio $K = \epsilon_\gamma \Omega_\gamma / \epsilon_\beta \Omega_\beta$ was measured with a source of Bi²⁰⁷ placed in the exact position occupied by

TABLE IV. Results of measurements on Ne¹⁸.

	Other authors	Our measurements
E_1	3.423 ± 0.020 MeV ^{a,c}	3.416 ± 0.009 MeV
E_2	2.382 ± 0.020 MeV ^{a,b,d}	2.373 ± 0.011 MeV ^d
E_γ ^e	1.041 ± 0.005 MeV ^{b,e} 1.043 ± 0.010 MeV ^f	1.030 ± 0.020 ^e
Half-life	1.46 ± 0.07 sec ^b	1.47 ± 0.10 sec
Branching ratio		
r_1	$(93 \pm 2)\%$	$(91 \pm 3)\%$
r_2	$(7 \pm 2)\%$	$(9 \pm 3)\%$
$\log f t_1$	3.049 ± 0.026 ^b	3.02 ± 0.02
$\log f t_2$	3.481 ± 0.110 ^b	3.47 ± 0.13
Mass excess of Ne ¹⁸	10.658 ± 0.010 MeV ^{a,f}	10.651 ± 0.010 MeV ^g

^a See Ref. 18.

^b See Ref. 12.

^c Value determined from the Q value of the O¹⁶(He³,n)Ne¹⁸ reaction.

^d Value calculated from the energy of the level reached in F¹⁸.

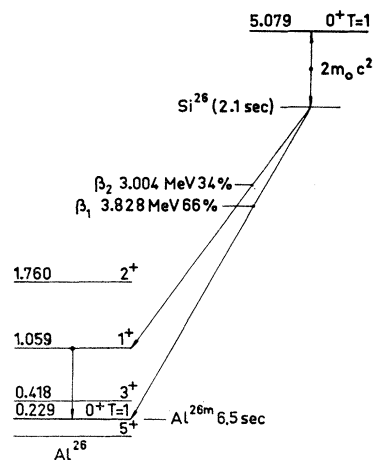
^e Energy of the gamma ray measured in the experiments on Ne¹⁸.

^f Energy of the F¹⁸ level reported in F. Ajzenberg-Selove and T. Lauritsen (Ref. 1).

^g Value determined by using E_1 and the mass excess of F¹⁸ 6.213 ± 0.004 MeV taken from Everling (see h below).

^h F. Everling, L. A. König, J. H. E. Mattauch, and A. H. Wapstra, Nucl. Phys. 18, 529 (1960).

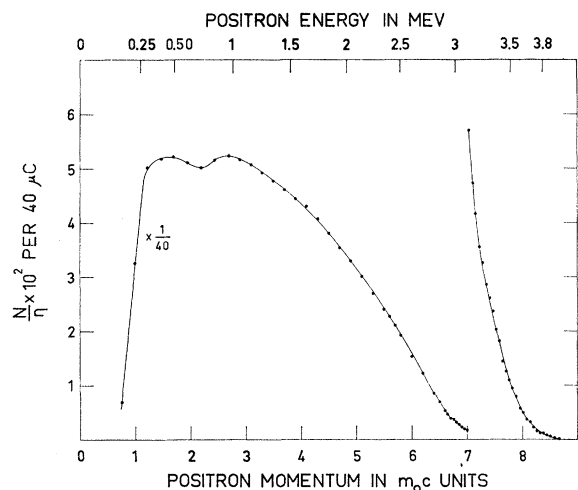
ⁱ D. E. Alburger and A. W. Sunyar, Phys. Rev. 99, 695 (1955).


 FIG. 13. Decay scheme of Si^{26} .

the target. This source emits internal conversion electrons and gamma rays of 1 MeV in a known ratio $\alpha = N_{0\beta}/N_{0\gamma} = 0.114$.²⁴ The number of counts in the photo peak of the 1 MeV γ ray is $N_{\gamma} = N_{0\gamma}\Omega_{\gamma}\epsilon_{\gamma}$ and the number of counts in the peak of the electron spectrum is $N_{\beta} = N_{0\beta}\Omega_{\beta}\epsilon_{\beta}$. We find $K = 0.114N_{\gamma}/N_{\beta} = 0.112$ in our case.

The calculation in this manner of the branching ratio for Ne^{18} gives us $r_1 = (91 \pm 3)\%$ and $r_2 = (9 \pm 3)\%$. The corresponding $\log ft$ values are 3.02 ± 0.02 , and 3.47 ± 0.13 , respectively. These results are in agreement with Butler and Dunning.¹²

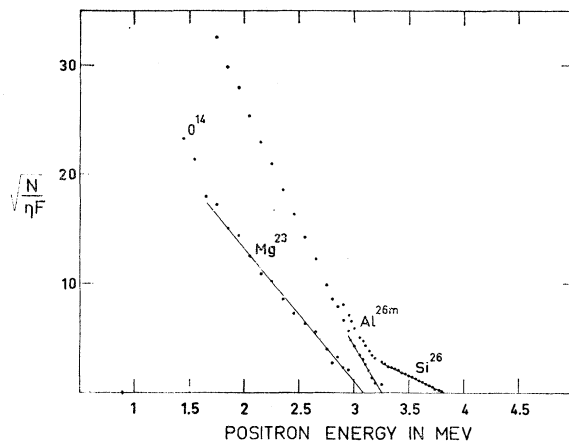
In summary, we have measured accurately the maximum energy of the beta-ray transition from Ne^{18} to the ground state of F^{18} and have determined the mass excess of Ne^{18} from this result. Our experiments confirm that the 1.04-MeV level in F^{18} is the $T=1$ analog of the ground state of Ne^{18} as previously deduced.^{12,13} Measurements of the various gamma-ray


 FIG. 14. Spectrum of positrons following the bombardment of a target of magnesium by He^3 ions ($E_b = 5$ MeV, beam intensity $0.5 \mu\text{A}$).

spectra allow us to fix upper limits of 1% on the positron branches to the 1.08-MeV ($J=0$) and 1.7-MeV ($J\pi = 1^+, T=0$) levels of F^{18} . Table IV shows our results compared with those of other authors.

Si^{26}

In order to study Si^{26} we used the reaction $\text{Mg}^{24}(\text{He}^3, n)\text{Si}^{26}$ occurring in the bombardment of a target of natural magnesium of 5 mg/cm^2 thickness with He^3 ions of 5-MeV energy. Table V shows the reactions that can occur. It is seen from the table that we can produce, aside from the Si^{26} which we are interested in, the positron-emitting isotopes Mg^{23} , Al^{25} , Al^{26} , Si^{27} . The spectra of positrons from these isotopes have maximum energies greater than 3 MeV. The carbon deposited on the target in the course of bombardment as well as oxygen contained in the oxide


 FIG. 15. Kurie plots obtained from the spectrum of positrons occurring in the bombardment of natural magnesium targets by He^3 ions. The various portions of the spectrum are assigned to Si^{26} , $E = (3.828 \pm 0.013)$ MeV, Al^{26m} , $E = (3.265 \pm 0.016)$ MeV and Mg^{23} , $E = (3.099 \pm 0.012)$ MeV.

layer moreover gives rise to the production of C^{11} , O^{14} , O^{15} , F^{18} , and Ne^{18} (see Tables I and III).

The measured spectra, one of which is given in Fig. 14, shows a maximum energy of about 3.7 MeV which corresponds to that seen previously in the spectra of Si^{26} and Si^{27} .

The Kurie-plot analysis of the spectrum (Fig. 15) shows for positrons of energies between 3.2 and 3.8 MeV a first branch having a maximum energy calculated to be $E_1 = (3.828 \pm 0.013)$ MeV taking into account a correction of 11 keV for the energy loss of electrons in the target. We assign the corresponding spectrum in this plot to the decay of Si^{26} to the 0.229-MeV isomeric state of Al^{26} . The points are on a straight line characteristic of an allowed transition. For those positrons of energies lower than 3.25 MeV we constructed a new Kurie plot and we find that these points are on a

TABLE V. Reactions due to the bombardment of a target of magnesium by He³ ions.^a

Abundance	Reactions		Half-life	E_{\max} MeV	Q
78.7%	Mg ²⁴ (He ³ , α)Mg ²³	β^+	12.04 \pm 0.09 sec	3.09 \pm 0.01 (95%) 2.65 \pm 0.01 (5%)	4.024 yes
	Mg ²⁴ (He ³ , t)Al ²⁴	β^+	2.09 \pm 0.04 sec	8.5	-14.04 no
	Mg ²⁴ (He ³ , d)Al ²⁵	β^+	7.23 \pm 0.03 sec	3.27 \pm 0.03	-3.206 yes
	Mg ²⁴ (He ³ , p)Al ^{26m}	β^+	6.47 \pm 0.06 sec	3.21 \pm 0.03	5.914 yes
	Mg ²⁴ (He ³ , n)Si ²⁶	β^+	2.1 \pm 0.3 sec	3.76	0.080 our study
10.1%	Mg ²⁵ (He ³ , α)Mg ²⁴	stable	13.24 no
	Mg ²⁵ (He ³ , t)Al ²⁵	β^+	7.23 \pm 0.03 sec	3.27 \pm 0.03	-4.279 no ^b
	Mg ²⁵ (He ³ , d)Al ^{26m}	β^+	6.47 \pm 0.06 sec	3.21 \pm 0.03	0.808 yes
	Mg ²⁵ (He ³ , p)Al ²⁷	stable	11.651 no
	Mg ²⁵ (He ³ , n)Si ²⁷	β^+	4.19 \pm 0.05 sec	3.820 \pm 0.050	6.054 yes
11.2%	Mg ²⁶ (He ³ , α)Mg ²⁵	stable	9.479 no
	Mg ²⁶ (He ³ , t)Al ^{26m}	β^+	6.47 \pm 0.06 sec	3.21 \pm 0.03	-4.032 no
	Mg ²⁶ (He ³ , d)Al ²⁷	stable	2.779 no
	Mg ²⁶ (He ³ , p)Al ²⁸	β^-	2.28 \pm 0.02 min	2.865 \pm 0.010	8.278 no
	Mg ²⁶ (He ³ , n)Si ²⁸	stable	12.13 no

^a These data have been taken from Endt and Van der Leun (Ref. 25). The remark "no" signifies that this reaction does not produce β^+ activities at the bombarding energy of 5.0 MeV. The remark "yes" signifies that such isotopes ought to be produced and that we should take them into account in the interpretation of our experiments.

^b The threshold for this reaction is at $E_{\text{He}^3} = 4.9$ MeV.

straight line between 3.1 and 3.25 MeV. The calculation of the maximum energy is $E = (3.265 \pm 0.016)$ MeV, a value which lies between the energies (3.210 ± 0.030) MeV and (3.270 ± 0.030) MeV reported for the positron decays of Al^{26m} and Al²⁵.

If we subtract from the experimental spectrum the activities calculated corresponding to these two groups we are able to construct a third Kurie plot having a maximum energy of (3.099 ± 0.012) MeV. We assign this branch to the positron decay of Mg²³ to the ground state of Na²³ which has been reported to have a maximum energy of (3.090 ± 0.010) MeV. We notice that the plot increases for those positron energies lower than 2 MeV. This corresponds to the presence of positrons associated with C¹¹, O¹⁴, O¹⁵, and F¹⁸, isotopes due to contaminants in the target.

We measured the decay of the intensity of positrons for different settings of the spectrometer. Thus, for 3.31 and 3.34 MeV, we find, respectively, $T_{1/2} = (2.2 \pm 0.2)$ sec and (2.1 ± 0.2) sec, each of these results being the average of 20 individual measurements. These values are in good agreement with the half-life $T_{1/2} = (2.1 \pm 0.3)$ sec reported by Robinson and Johnson²⁰ for Si²⁶. Table V shows, however, that in this energy region we ought to observe positrons due to Si²⁷ (4.19 sec, 3.82 MeV) produced in the reaction Mg²⁵(He³, n)Si²⁷.

The errors in our measurement of the half-life allows us to set a maximum of 15% for the relative contribution of Si²⁷ in the spectrum measured at 3.3 MeV.

In that portion of the spectrum assigned to Al^{26m} in Fig. 15, we measured a half-life of (3.4 ± 0.1) sec for the decay of positrons of 3.27 MeV. This value results from the simultaneous presence of positrons due to Si²⁶ (+Si²⁷) and to another isotope. Since we know the relative intensities of the different branches for this energy we can deduce the half-life of the other isotope.

We find for the other isotope $T_{1/2} = 6.5$ sec which corresponds to the value reported by Endt²⁵ for Al^{26m}, namely $T_{1/2} = 6.47$ sec. However, we are not able to exclude the presence in the source of the isotope Al²⁵ (7.23 sec).

For the energies of positrons lower than 3.1 MeV, we find even longer half-life values which indicates that the spectrum contains a component resulting from another isotope which we already identified with Mg²³ by making a Kurie-plot analysis. Robinson and Johnson²⁰ have reported a positron branch due to the decay of Si²⁶ to the 1.059-MeV excited state of Al²⁶. The maximum energy of these positrons should be about 3.0 MeV. Since it follows from our measurements that this positron branch cannot be observed, the corresponding Kurie plot is confused with that due to the positron activity of Mg²³. We have been able to establish the presence of this group by measurements on the decay of positrons of selected energy using the spectrometer at energies between 2 and 3 MeV. We carried out these measurements every 50 keV. For a given value of the energy the Kurie-plot analysis gives us the intensity of each branch of the spectrum and we can deduce a half-life corresponding to a branch of maximum energy 3.1 MeV. If the spectrum corresponding to this end point were due uniquely to the decay of Mg²³ we ought to find $T_{1/2} = 12$ sec, a value reported for Mg²³. In fact we always find smaller values, which leads us to believe that a portion of the spectrum was due to positrons from the decay of Si²⁶ to the 1.059-MeV excited state in Al²⁶. The value measured experimentally together with the known values of the half-lives of Mg²³ and Si²⁶ then allows us to deduce the relative intensities of each of these two

²⁵ P. M. Endt and C. Van der Leun, Nucl. Phys. **34**, 1 (1962).

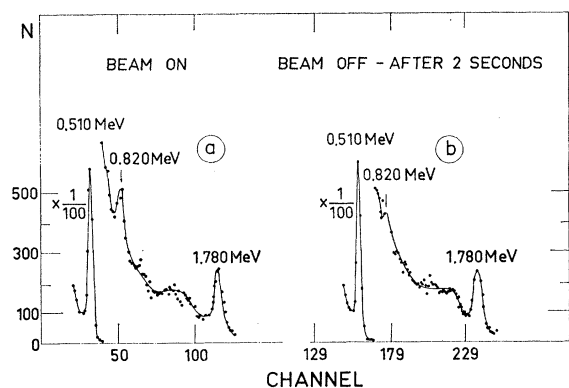


FIG. 16. Gamma-ray spectra following the He^3 bombardment of a magnesium target. Curve (a) shows a spectrum observed with a circuit programmer for a source in radioactive equilibrium. In addition to the intense 0.510-MeV gamma rays one line is seen at 0.820 MeV and another at 1.780 MeV. Curve (b) shows the same spectrum after the beam has been cut off for 2 sec. The line at 0.820 MeV has diminished in intensity whereas the others have not changed. The gamma ray of 0.820 MeV is assigned to the decay of the 1.059-MeV level of Al^{26} fed in the β^+ radioactivity of Si^{26} . A gamma ray of 1.780 MeV is due to the decay of the 1.77-MeV level in Si^{28} fed in the β^- radioactivity of Al^{28} (2.28 min).

isotopes. We thus find that $(7 \pm 1)\%$ of this intensity is due to positrons from the second branch of Si^{26} . This result permits us to determine the branching ratios of Si^{26} . In order to do so we compared the area A_1 of the spectrum calculated according to the Kurie plot of maximum energy 3.8 MeV and the area A_2 due to the

TABLE VI. Results of measurements on Si^{26} .

	Other authors	Our measurements
E_1	3.80 MeV ^{a,f}	3.828 ± 0.013 MeV
E_2	$3.80 - 0.83 = 2.97^{\text{a,b,g}}$	3.008 ± 0.015 MeV ^e
E_γ	$0.824 \pm 0.015^{\text{b}}$ $0.830 \pm 0.003^{\text{e}}$	0.820 ± 0.010 MeV
Half-life	2.1 ± 0.3 sec ^b	2.1 ± 0.1 sec
Branching ratio		$r_1 = \begin{pmatrix} 66 & +1 \\ & -4 \end{pmatrix} \%$ $r_2 = \begin{pmatrix} 34 & +4 \\ & -1 \end{pmatrix} \%$
$\log ft_1$...	$3.52^{+0.04}_{-0.02}$
$\log ft_2$		$3.36^{+0.02}_{-0.05}$
Mass excess of Si^{26}	(0.55 ± 0.08) MeV ^{a,f}	0.574 ± 0.013 MeV ^h
$E \text{ Al}^{26m}$	3.210 ± 0.030 MeV ^d	3.265 ± 0.016 MeV ⁱ
$E \text{ Mg}^{23}$	3.090 ± 0.010 MeV ^e	3.099 ± 0.012 MeV ⁱ

^a See Ref. 16.
^b See Ref. 20.
^c See Ref. 25.
^d B. Elbek, B. S. Madsen, and O. Nathan, *Phil. Mag.* **46**, 663 (1955).
^e R. Wallace and J. A. Welch, Jr., *Phys. Rev.* **117**, 1297 (1960).
^f Value determined by the measurement of the Q value of the $\text{Mg}^{24}(\text{He}^3, n)\text{Si}^{26}$ reaction.
^g Value calculated according to the energy of the level reached in Al^{26} .
^h Value determined according to E_1 and the mass excess of Al^{26} (see Ref. 25).
ⁱ These results are disturbed by the presence of isotopes in this neighborhood.

plot of maximum energy 3.1 MeV. The branching ratios are equal to $r_1 = A_1/A_1 + 0.07A_2$ and $r_2 = 0.07A_2/A_1 + 0.07A_2$. We thus find $r_1 = (66_{-4}^{+1})\%$ and $r_2 = (34_{-1}^{+4})\%$. The errors take into account the 15% contribution due to Si^{27} in the area A_1 . This calculation can be relied upon only if the decay scheme proposed by Robinson is correct and if in the target there do not exist activities having half-lives of less than 12 sec other than those cited in this discussion. We have been able to confirm the existence of this Si^{26} branch to an excited state of Al^{26} by the observation of a gamma ray of (0.820 ± 0.010) -MeV energy. By means of the programming circuit (Fig. 16) we were able to show that the intensity of this line decays with a half-life of (2.0 ± 0.4) sec. Since Si^{26} is the only isotope produced with a half-life of this order of magnitude we assign this gamma ray to the decay of the 1.059-MeV level of Al^{26} fed in the positron decay of Si^{26} and de-exciting to the isomeric level in Al^{26} at 0.229 MeV.

In this same spectrum we see a line at 1.8 MeV whose intensity does not decay very much after cutting off the beam for several seconds. We assign this line to the beta decay of Al^{28} to the first excited state in Si^{28} at 1.77 MeV.²⁵ Al^{28} has a half-life of 2.3 min and is produced by the reaction $\text{Mg}^{26}(\text{He}^3, p)\text{Al}^{28}$. By means of measurements on the positrons with scintillation detectors in a manner analogous to that described in the study of Ne^{18} , we determined the branching ratios of Si^{26} . We find $r_1 = (60 \pm 5)\%$ for the more energetic branch and $r_2 = (40 \pm 5)\%$ for the second branch. The results are consistent with those determined above by means of the magnetic spectrometer and by the half-lives.

In summary our experiments have shown that Si^{26} decays to Al^{26} with the emission of two positron branches, one to the 0.229-MeV isomeric level with a

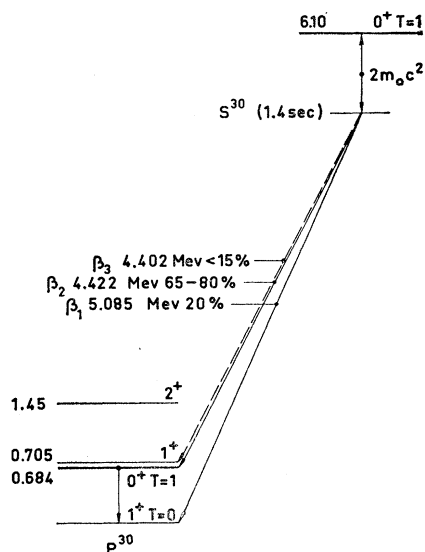


FIG. 17. Decay scheme of S^{30} .

TABLE VII. Reactions due to a bombardment of a target of natural silicon by He³ ions.^a

Abundance			Half-life	E_{\max} MeV	Q MeV	Remarks
92.2%	Si ²⁸ (He ³ , α)Si ²⁷	β^+	4.19 \pm 0.05 sec	3.820 \pm 0.050	3.399	yes
	Si ²⁸ (He ³ , t)P ²⁸	β^+	0.28 sec	10.6	-13.82	no
	Si ²⁸ (He ³ , d)P ²⁹	β^+	4.23 \pm 0.05 sec	3.945 \pm 0.005	-2.746	yes
	Si ²⁸ (He ³ , p)P ³⁰	β^+	2.55 \pm 0.02 min	3.240 \pm 0.040	6.344	yes
	Si ²⁸ (He ³ , n)S ³⁰	β^+	1.35 \pm 0.1 sec	4.3, 4.98	0.410	yes our study
4.7%	Si ²⁹ (He ³ , α)Si ²⁸	stable	12.10	no
	Si ²⁹ (He ³ , t)P ²⁹	β^+	4.23 \pm 0.05 sec	3.945 \pm 0.005	-4.966	no
	Si ²⁹ (He ³ , d)P ³⁰	β^+	2.55 \pm 0.02 min	3.240 \pm 0.040	0.091	yes
	Si ²⁹ (He ³ , p)P ³¹	stable	10.18	no
	Si ²⁹ (He ³ , n)S ³¹	β^+	2.61 \pm 0.03 sec	4.390 \pm 0.030	3.951	yes
3.1%	Si ³⁰ (He ³ , α)Si ²⁹	stable	9.962	no
	Si ³⁰ (He ³ , t)P ³⁰	β^+	2.55 \pm 0.02 min	3.240 \pm 0.040	-4.266	yes
	Si ³⁰ (He ³ , d)P ³¹	stable	1.793	no
	Si ³⁰ (He ³ , p)P ³²	β^-	14.32 \pm 0.02 days	1.709 \pm 0.001	7.505	no
	Si ³⁰ (He ³ , n)S ³²	stable	8.430	no

^a These values were taken from Ref. 25. The remark "no" signifies that this reaction does not produce β^+ activities at the bombarding energy of 5.4 MeV. The remark "yes" signifies that these isotopes could be produced and that we should take them into account in the interpretation of our experiments.

maximum energy of (3.828 \pm 0.013) MeV and the other to the 1.059-MeV excited state with a maximum energy of (3.008 \pm 0.015) MeV. The corresponding $\log ft$ values are (3.52 $_{-0.02}^{+0.04}$) and (3.36 $_{-0.05}^{+0.02}$), respectively. The ground state of Si²⁶ ($J^\pi=0^+$), the 0.229-MeV level of Al²⁶ ($J^\pi=0^+$) and the ground state of Mg²⁶ form a $T=1$ isobaric triplet. The positron transition to the 0.229-MeV state is pure Fermi while the transition to the 1.059-MeV level in Al²⁶ is pure Gamow-Teller.

The complete results listed in Table VI are in agreement with those of other authors.

S³⁰

We used the reaction Si²⁸(He³, n)S³⁰ for the study of the radioactivity of S³⁰. Aside from this reaction, the

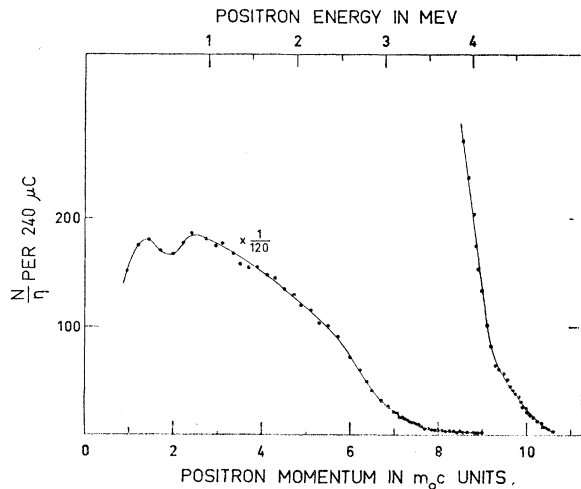


FIG. 18. Spectrum of positrons following the bombardment of a target of silicon with He³ ions ($E_b=5.4$ MeV, beam intensity 0.5 μ A).

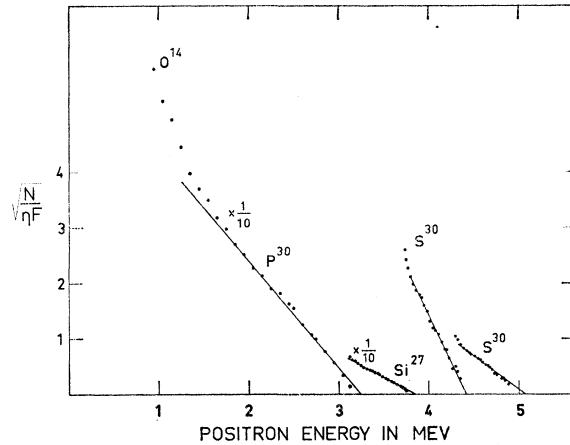


FIG. 19. Kurie-plot analysis of the spectrum of positrons following the bombardment of a silicon target by He³ ions. One sees the plots corresponding to the branches of S³⁰, $E_1=(5.085 \pm 0.026)$ MeV and $E_2=(4.422 \pm 0.022)$ MeV, of Si²⁷, $E=(3.852 \pm 0.016)$ MeV, of P³⁰, $E=(3.245 \pm 0.025)$ MeV.

bombardment of a target of natural silicon containing 92.2% Si²⁸, 4.7% Si²⁹, and 3.1% Si³⁰ leads to numerous other reactions which we have listed in Table VII. The bombarding energy was 5.4 MeV.

Just as in the preceding experiments we took into account the reactions due to the presence of carbon and oxygen in the target. The isotopes produced by these reactions however did not interfere provided we used only that portion of the spectrum above 2 MeV. Table VII shows that in our discussions we have to take into account Si²⁷, P²⁹, P³⁰, and S³¹. We measured many spectra one of which is shown in Fig. 18.

The results of these measurements have been analyzed by making Kurie plots (Fig. 19). For positron energies between 4.4 and 5 MeV, we find a straight-line

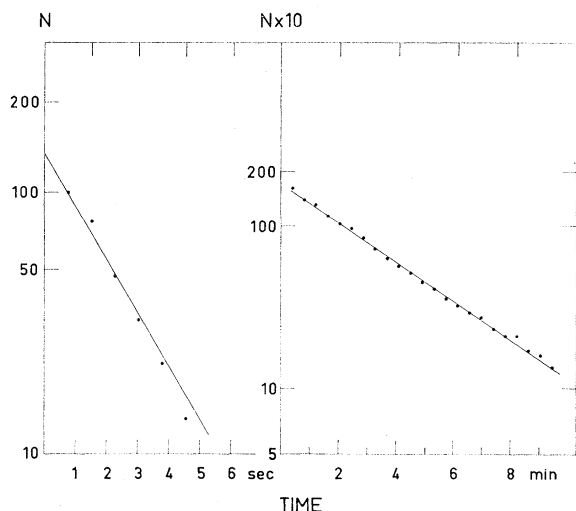


FIG. 20. (a) Half-life of S^{30} determined from the decay of positrons at a focusing energy of 3.9 MeV; $T_{1/2} = 1.4 \pm 0.1$ sec. (b) Half-life of P^{30} determined from the decay of the positrons at a focusing energy of 2.5 MeV; $T_{1/2} = 2.6 \pm 0.1$ min.

plot. The maximum energy of this branch calculated by the method of least squares is equal to (5.085 ± 0.026) MeV (taking into account an absorption in the target amounting to 5 keV). We identify this branch as a positron transition of S^{30} to the ground state of P^{30} . After subtracting the spectrum corresponding to this first branch we find a straight line for a new Kurie plot between 3.8 and 4.4 MeV. This branch has an end-point energy of (4.422 ± 0.022) MeV. We can assign this to the positron decay of S^{30} to the 0.684-MeV level of P^{30} . However, this measurement alone does not allow us to exclude the presence in the target of P^{29} (3.945 MeV) and S^{31} (4.390 MeV). After subtraction of these first two groups from the total spectrum the remainder gives another straight-line Kurie plot extending from 3.2 to 3.8 MeV having an end-point energy of (3.852 ± 0.016) MeV. This value compares with that reported for Si^{27} , namely (3.820 ± 0.050) MeV, and we are able to assign this branch to the positron decay of Si^{27} to the ground state of Al^{27} . Finally, in region of energies below 3.2 MeV we can construct another Kurie plot of maximum energy (3.245 ± 0.025) MeV. We assign this to the positron decay of P^{30} to the ground state of Si^{30} . This last plot shows for positron energies lower than 2 MeV an increase which we attribute to the presence in the target of contamination isotopes of carbon and oxygen.

In this study we also measured the decay of positrons of 3.9-MeV energy selected by the spectrometer. The average of 120 individual measurements at this setting gives us $T_{1/2} = (1.4 \pm 0.1)$ sec [Fig. 20(a)]. This result is in agreement with the value of (1.35 ± 0.10) sec for the half-life of S^{30} reported by Robinson.²³ Taking into account the error in our measurement, we estimate that at a positron energy of 3.9 MeV the contribution

of P^{29} and/or S^{31} is less than 5% of the total intensity. In that portion of the spectrum corresponding to the Kurie plot marked Si^{27} in Fig. 19 we measured $T_{1/2} = (3.46 \pm 0.10)$ sec for positrons of 3.5 MeV. This value evidently results from the simultaneous presence of positrons due to S^{30} and to at least one other isotope. By knowing the relative intensities of the different branches at the energy in question, one can deduce the half-life of the unknown isotope. Proceeding in this way we have been able to establish that this isotope was Si^{27} . At energies below 3.2 MeV we found in addition to half-lives of the order of seconds, a half-life $T_{1/2} = (2.6 \pm 0.1)$ min [Fig. 20(b)], a value which is in agreement with that reported by other authors²⁵ for P^{30} ; (2.55 ± 0.02) min. We have thus identified the various components of the spectrum. A first part of maximum energy equal to 5.085 MeV corresponds to the decay of S^{30} to the ground state of P^{30} . The second group which ends at 4.422 MeV, is due to the decay of S^{30} to an excited state of P^{30} whose energy is $5.085 - 4.422 = (0.663 \pm 0.034)$ MeV. The remaining two groups are due to the positron decays of Si^{27} and P^{30} . By means of Kurie-plot analyses we have determined relative intensities of $(20 \pm 1)\%$ for the branch to the ground state of P^{30} and $(80 \pm 1)\%$ for the transitions to one or both of the two excited states at 0.684 MeV and at 0.704 MeV. The errors take into account the contributions of P^{29} and S^{31} in the experimental spectrum.

The gamma-ray spectrum shows a line of (0.687 ± 0.005) MeV. By means of the circuit programmer we have shown that this line decays with a half-life of (1.2 ± 0.2) sec (Fig. 21). Since S^{30} is the only isotope present with a half-life of this order of magnitude, we have assigned this line to the decay of a level of P^{30}

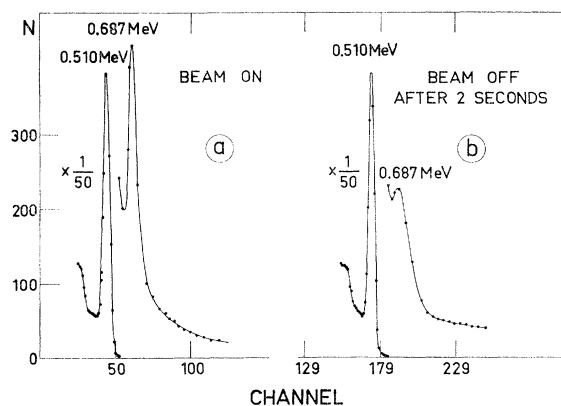


FIG. 21. Spectra of gamma rays following the He^3 bombardment of silicon. Curve (a) shows a spectrum obtained with the circuit programmer for a source in radioactive equilibrium. Aside from the intense 0.510-MeV gamma rays another line is seen at 0.687 ± 0.005 MeV. Curve (b) shows the same spectrum after the beam has been cut off for 2 sec. The line at 0.687 MeV has diminished in intensity. This gamma ray is assigned to the de-excitation of a level of P^{30} fed in the β^+ radioactivity of S^{30} .

fed in the positron decay of S³⁰. The combination of these results allows us to say that the inner beta-ray group decays mainly to the (0.684±0.003)-MeV level of P³⁰ reported by Endt.²⁵

Our results do not allow us to say whether or not a third branch in the decay of S³⁰ feeds the 0.704-MeV (*J*^π=1⁺) level of P³⁰. However, an analysis of the shape of the 0.687-MeV photopeak leads to the conclusion that this third branch, if it exists, has an intensity of <15%. The values of the branching ratios are therefore *r*₁=(20±1)%₀, *r*₂=(80⁺¹₋₁₅)%₀ and *r*₃<15%₀ and the *log ft* values are (4.39±0.03), (3.49^{+0.09}_{-0.03}) and >4.21, respectively.

Our results compared with those of other authors are listed in Table VIII. The transition to the ground state

 TABLE VIII. Results of measurements on S³⁰.

	Other authors	Our measurements
S ³⁰		
<i>E</i> ₁	4.980±0.150 MeV ^{a,d}	5.085±0.026 MeV
<i>E</i> ₂	4.300±0.150 MeV ^{a,e} 4.220±0.150 MeV ^{b,e}	4.422±0.022
(<i>E</i> ₃)	(4.280±0.150 MeV) ^{a,f}	(4.402±0.022 MeV) ^f
<i>E</i> ₁ − <i>E</i> ₂	0.677±0.010 MeV ^{a,g} 0.676 ^{b,g} 0.684±0.003 MeV ^{c,h}	0.687±0.005 MeV ^g 0.663±0.034 MeV ⁱ
Half-life	1.35 ±0.1 sec ^a 1.5 ±0.1 sec ^b	1.4 ±0.1 sec
Branching ratio		
1	(19±2)% ^{a,i}	(20±1)% ₀
2	(73±7)% ₀	(80 ⁺¹ ₋₁₅)% ₀
3	(8±10)% ₀	<15% ₀
<i>log ft</i> ₁	4.37 ^j	4.39 ±0.03
<i>log ft</i> ₂	3.5	3.49 ^{+0.09} −0.03
<i>log ft</i> ₃	4.46	>4.21
Mass excess	−(5.340±0.110) MeV ^{e,k}	−(5.205±0.026) MeV ^l
Si ²⁷		
<i>E</i> ₀	3.820±0.050 MeV ^e	3.852±0.016 MeV
<i>T</i>	4.19 ±0.05 sec ^e	...
P ³⁰		
<i>E</i> ₀	3.240±0.040 MeV ^e	3.245±0.025 MeV
<i>T</i>	2.55 ±0.02 min	2.6 ±0.1 min

^a See Ref. 23.

^b See Ref. 22.

^c See Ref. 25.

^d Value not measured, deduced from the value of *E*₂.

^e Value measured by means of scintillation detectors.

^f This branch has not been observed—the energy has been calculated according to that given from levels of P³⁰.

^g Energy of the gamma ray in cascade with the radioactivity of P³⁰.

^h Energy of the level reported by Endt (Ref. 25).

ⁱ Value determined according to the maximum energies of the positron spectra.

^j Values determined by theoretical considerations.

^k Value calculated according to the energies of the β⁺ transitions of S³⁰ (Refs. 22 and 23).

^l Value calculated by using a value of (11.312±0.009 MeV) for the mass excess of P³⁰.

of P³⁰ is pure Gamow-Teller ($\Delta J=1$), while that to the 0.684-MeV state is pure Fermi. The *log ft* value for the latter transition is equal within the limits of error to the values determined for other transitions of the same character, notably for O¹⁴. The ground state of S³⁰ (*J*^π=0⁺), the 0.684-MeV level of P³⁰ and the ground state of Si³⁰ form an isobaric triplet.

DISCUSSION

Apart from the improvement of our systematic knowledge of beta-decay the chief results of these investigations have been

- (i) The confirmation that the ground-state transition in the beta decay of O¹⁴ takes place and the determination of its *log ft* value as 7.23±0.04.
- (ii) The determination of the *log ft* values for the beta decay of Ne¹⁸, Si²⁶, and S³⁰ to the analog *T*=1 states of F¹⁸, Al²⁶, and P³⁰ at 1.043, 0.229, and 0.684 MeV as 3.47±0.13, 3.52_{-0.02}^{+0.04} and 3.49^{+0.09}_{-0.03}, respectively.

On the first point we may repeat the old comment that the large *log ft* value (9.0) for the beta-decay of C¹⁴ is due to an accidental cancellation of terms in the matrix element. The still large but substantially smaller *log ft* for the mirror decay of O¹⁴ that we confirm and present here then must reflect the partial undoing of this chance cancellation by the charge-dependent effects that distinguish in detail the ground-state wave functions of C¹⁴ and O¹⁴. While we have no exact account of the origin of the cancellation we cannot discuss in detail its change in going from C¹⁴ to O¹⁴. Note however, that, given the C¹⁴ and N¹⁴ (ground-state) wave functions, the O¹⁴ decay limits the charge dependence that we may assume to obtain in the nuclear force. This comparison between the C¹⁴ and O¹⁴ beta decay may then become useful in discussing the difference between the wave functions of O¹⁴ and its analog, the first *T*=1 state at 2.31 MeV, in N¹⁴ that is crucial for testing of the hypothesis of the conserved vector current²⁶ by comparing the O¹⁴ and μ-meson lifetimes.^{8,9} We are not yet able to take advantage of this possibility.

The second of the two points listed above also concerns the conserved vector current. The three transitions in question are all of the pure Fermi (vector) type and so should show identical *log ft* values with that for the decay of O¹⁴ to its analog state (3.488±0.002) if the vector current is conserved (leaving out of account small changes due to differing radiative corrections in the various cases). If the vector current were “completely nonconserved” in the sense that the pions were completely uncoupled to the lepton field we

²⁶ R. P. Feynmann and M. Gell-Mann, Phys. Rev. **109**, 193 (1958).

should probably expect²⁷ substantially bigger differences between the $\log ft$ values for these Fermi transitions than we find here.

²⁷ R. J. Blin-Stoyle, V. Gupta, and J. S. Thomson, Nucl. Phys. 14, 685 (1959).

ACKNOWLEDGMENTS

Two of us (D. E. A. and D. H. W.) are indebted to Professor S. Gorodetzky for the opportunity of participating in this research as visitors at the Institute of Nuclear Research.

Moments of Inertia and the Shell Model*

C. A. LEVINSON

Department of Nuclear Physics, The Weizmann Institute of Science, Rehovoth, Israel

(Received 1 July 1963)

The variational formula of Skyrme for the moment of inertia is analyzed in some detail. The errors in this formula are studied and an upper bound is given. It is found that in the case of the shell model this approach is quite accurate and allows use of general Hamiltonians.

I. INTRODUCTION

THE general problem of using shell-model techniques for investigating collective properties of nuclei is a challenging one whose solution will certainly lead to a more fundamental understanding of collective nuclear models. In a previous paper¹ the emphasis was on the connection between the shell model and the vibrational model.

However, there is a broad class of nuclei with clearly defined rotational properties for low excitation energies whose vibrational levels lie much higher in energy. These are the so-called "strongly deformed" nuclei and the natural parameter describing their low excited states is the moment of inertia. The question considered in this paper is the following: Given a shell-model single-particle well and two-body interaction, how does one go about computing the moment of inertia? One solution that comes to mind is to set up some kind of Hartree-Fock scheme using the given Hamiltonian and then apply the Inglis² "cranking formula" for the evaluation of the moment of inertia. Indeed, Nilsson and Prior³ have carried out such a program where instead of a Hartree-Fock calculation they calculated the wave functions using a given single-particle deformed field plus a pairing force. This approach has been fairly successful. However, in characterizing the underlying shell-model Hamiltonian only in terms of a pairing part and a single-particle deformed well one loses some control of the problem and any systematic disagreements between the theoretical calculations and experiment are

hard to study since modifications of the underlying interaction are quite difficult to make. On the other hand, the degree of validity of the cranking formula itself is hard to assess in a real nucleus. In addition, it is not clear that the Nilsson and Prior approach will work at all well for the light-deformed nuclei where pairing theory has not been successfully applied.

Let us review the possibilities open to us if we wish to use a given shell-model Hamiltonian for our calculation. First, consider the Hartree-Fock problem. In general, this is quite difficult since the orbitals can be varied quite arbitrarily. However, if we restrict the possible variations so that the orbitals retain axial symmetry and are made up of components from a single major shell then the resulting calculations are quite feasible. Possibly one can even go farther and include pairing-type degrees of freedom by working with "quasiparticles."

The next problem that arises is how to extract the moment of inertia from these wave functions and the Hamiltonian. Exploratory calculations using the "cranking formula" in the s - d shell indicated insufficient accuracy in cases where one knew beforehand the actual eigenvalues of the Hamiltonian. On the other hand, the variational formula of Skyrme⁴ worked out quite well in these cases. This was indeed encouraging and led to a further analysis of this approach. In this paper the problem of finding a variational formula for the moment of inertia under our self-imposed shell-model boundary conditions is investigated. In addition, the accuracy of the final formula is given in terms of an upper bound on the error. The final result presented is, indeed, Skyrme's formula.

For even-even nuclei one thus has a fairly accurate feasible method for computing deformed wave functions and moments of inertia from a given shell-model

* The research reported in this document has been sponsored in part by Office of Scientific Research OAR, through the European Office, Aerospace Research, U. S. Air Force.

¹ E. Flamm, C. A. Levinson, and S. Meshkov, Phys. Rev. 129, 297 (1963).

² D. Inglis, Phys. Rev. 96, 1059 (1959).

³ S. G. Nilsson and O. Prior, Kgl. Danske Videnskab. Selskab, Mat Fys Medd. 32, No. 16 (1960).

⁴ T. H. R. Skyrme, Proc. Phys. Soc. (London) A70, 433 (1957).